Accepted Manuscript

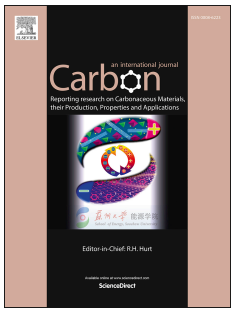

Fabrication of Three Terminal Devices by ElectroSpray Deposition of Graphene Nanoribbons

P. Fantuzzi, L. Martini, A. Candini, V. Corradini, U. del Pennino, Y. Hu, X. Feng, K. Müllen, A. Narita, M. Affronte

PII: S0008-6223(16)30241-X

DOI: 10.1016/j.carbon.2016.03.052

Reference: CARBON 10874

To appear in: *Carbon*

Received Date: 8 January 2016

Revised Date: 18 March 2016

Accepted Date: 23 March 2016

Please cite this article as: P. Fantuzzi, L. Martini, A. Candini, V. Corradini, U. del Pennino, Y. Hu, X. Feng, K. Müllen, A. Narita, M. Affronte, Fabrication of Three Terminal Devices by ElectroSpray Deposition of Graphene Nanoribbons, *Carbon* (2016), doi: 10.1016/j.carbon.2016.03.052.

Fabrication of Three Terminal Devices by ElectroSpray Deposition of Graphene Nanoribbons

P. Fantuzzi[1,2,*], L. Martini[1,2], A. Candini[2], V. Corradini[2], U. del Pennino[1,2], Y. Hu[3], X. Feng[4], K. Müllen[3], A. Narita[3], M. Affronte[1,2].

[1] Dipartimento di Scienze Fisiche, Informatiche e Matematiche, Università di Modena eReggio Emilia, Via G.Campi 213/a – 41125 Modena – Italy

[2] Centro S3 - Istituto di Nanoscienze - CNR, Via G. Campi 213/a - 41125 Modena – Italy

[3] Max Planck Institute for Polymer Research, Ackermannweg 10, D-55128 Mainz, Germany

[4] Center for Advancing Electronics Dresden (CFAED) & Department of Chemistry and Food Chemistry, Technische Universität Dresden, 01062 Dresden, Germany

Abstract

Electrospray deposition (ESD) in ambient conditions has been used to deposit graphene nanoribbons (GNRs) dispersed in liquid phase on different types of substrates, including ones suitable for electrical transport. The deposition process was controlled and optimized by using Raman spectroscopy, Scanning Probe Microscopy and Scanning Electron Microscopy. When deposited on graphitic electrodes, GNRs were used as semi-conducting channel in three terminal devices showing gate tunability of the electrical current. These results suggest that ESD technique can be used as an effective tool to deposit chemically synthesized GNRs onto substrates of interest for technological applications.

* Corresponding author at: Dipartimento di Scienze Fisiche, Informatiche e Matematiche, Università di Modena e Reggio Emilia, Via G. Campi 213/a, 41125 Modena, Italy.
E-mail address: paolo.fantuzzi@unimore.it (P. Fantuzzi)

1.Introduction

The use of graphene in electronics is attracting much interest for its potential as constituent material of several devices like transistors, sensors, touch screens and energy storage devices [1]. Its excellent charge mobility and transparency to the visible light are well established and ready to be exploited, but the use of graphene in electronic devices, such as a field effect transistor (FET), requires the presence of an energy gap in the electronic band structure and viable strategies to achieve this goal are still under exploration. The reduction of the lateral size of the graphene layers down to nanoribbons (GNRs) with nm-sized width is an efficient way to induce an energy gap, however as long as the GNRs are obtained by conventional top-down approaches such as lithography [2] or by unzipping of carbon nanotubes [3], the resulting structure is not controllable, making the electronic properties unpredictable. The use of chemically synthesized GNRs with atomically-controlled width is therefore very appealing in this context. Typically, high-quality GNRs are grown in ultra high vacuum on metallic surfaces [4,5], whereas a non-conducting substrate is mandatory for applications in electronics. GNRs with atomically defined edges can be alternatively synthesized in liquid-phase [6,7]. Given their huge mass, they cannot be evaporated and the deposition is usually performed by drop casting, possibly functionalizing the surface of insulating substrates [8-10].

Electrospray deposition (ESD) [11-15] is an alternative technique that allows to softly land large and heavy molecules from liquid suspension on to any substrate. ESD has been successfully used for the deposition of giant biomolecules (proteins) [16], fullerenes [17,18], carbon nanotubes [19], molecular nanomagnets [20-23] and nanoparticles [24], thus enabling integration of large molecular units in electronic circuits. Homemade and commercial apparatuses are proposed for ESD in a large variety of design and sophistication. Briefly, besides the capillary injecting the desired sprayed solution/suspension and the target holding the desired support, an ESD setup may include: 1) stages under differential pressure, leading to an UHV environment where the support (either conducting or insulator) is maintained; 2) one or more stages of electromagnetic lenses that act as mass selectors and/or to (de-)accelerate molecules.

Here we report a feasibility study for the fabrication of three terminal electronic devices made of chemically synthesized GNRs dispersed in tetrahydrofuran (THF) and deposited by an elementary ESD setup. The idea is to use *jugaad* approach to test the viability of this route. To this end, we control the morphology of the deposited GNR film by optical microscopy, scanning electron microscope (SEM), atomic force microscopy (AFM), scanning tunneling microscopy (STM) and the quantity of deposited material by Raman spectroscopy. To prove the effectiveness of our approach, GNRs have been deposited on graphitic electrodes and the *I-V* characteristics measured at room temperature show a pronounced gate tunability of the device current.

2. Experimental Methods

2.1 Electro spray apparatus

The ESD system used in our experiments is the early stage of a *Thermo Finnigan Surveyor* Mass Spectrometer (MSQ). The quadrupole and the mass analyzer stage were not used due to the huge mass of the GNRs (molecular weight in the order of 10^4–10^5 a.u.). Briefly (see Fig.1), our Electrospray source is composed by a stainless steel capillary where the solution flows. The capillary can be hold at a voltage V_c, tunable in the range ± 5 kV, with respect to the target and the rest of the chamber. It is surrounded by a tube injecting nitrogen and the action of both the gas and the applied voltage V_c produce an aerosol of liquid droplets [25]. The pressure of the nitrogen gas was kept at 4 bar at the entrance of the tube in order to get high flux of clean nitrogen in the whole deposition chamber. The solution is initially contained in an external syringe and driven into the capillary by a pump.

The capillary and its casing can be heat up to 650°C. High temperature facilitates the evaporation of the solvent and impedes the blocking of the capillary due to the accumulation of agglomerates. The quantity of solute actually deposited on substrate was controlled by the time of surface exposure and, indirectly, by the concentration of the solution, while the rate of the syringe pump was kept constant. All the depositions have been carried out in ambient conditions, namely the substrate was kept at room temperature and exposed to atmospheric pressure.

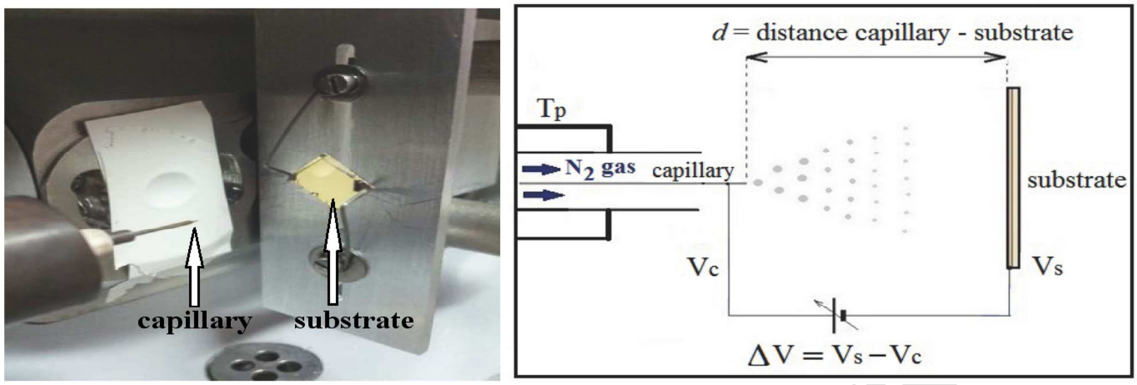

Figure 1: Scheme of the ESD system with the relevant parameters: the probe temperature (T_p), the capillary voltage (V_c) and that of the substrate (V_s) and the distance between substrate and capillary (d).

2.2 Graphene nanoribbons and their dispersion

In this work we have used structurally well-defined GNRs with a "cove"-type edge structure and width of approximately 1nm (Fig. 2). They exhibit a semiconducting behavior with 1.88 eV optical band-gap [6]. They are bottom-up synthesized by the methods of synthetic organic chemistry, following the procedure reported in Ref.[6]. Briefly, the synthesis was carried out through the AB-type Diels-Alder polymerization of a monomeric precursor 2,5-bis-(4-dodecylphenyl)-3-(3-ethynylphenyl)-4-phenyl-2,4-cyclopentadienone to provide non-planar polyphenylene precursors, which were subsequently "graphitized" by oxidative cyclodehydrogenation in solution. Uniform GNRs with the same width and edge structure have thus obtained as powder samples, which could be dispersed in organic solvents such as THF, thanks to the fact that they possess dodecyl ($C_{12}H_{25}$) chains attached at the peripheral positions. Relatively short GNR samples (≈100 nm, nominally) have been used for our ESD experiments, considering the decreasing dispersibility of longer GNRs. The average lengths were estimated by molecular modeling and by weight-average molecular weights of the corresponding polyphenylene precursors, obtained by the gel permeation chromatography analyses against polystyrene standards. For sake of completeness we just mention that two other GNR samples with different lengths, respectively ≈ 20 and

80 nm, have been also deposited and they gave quite similar results, at least within our analysis.

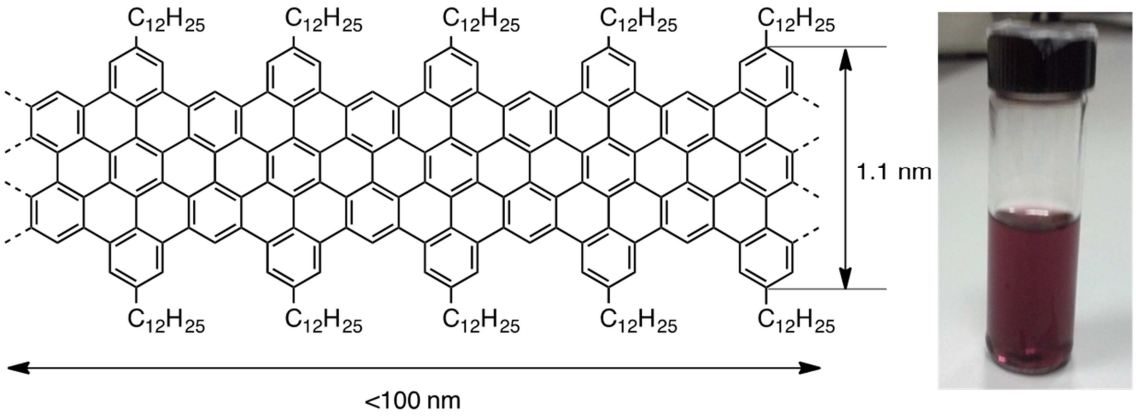

Figure 2: Left: Chemical structure of the GNRs used for the depositions. Right: Mother dispersion S_0 of the GNRs in THF.

In the following, we define "mother dispersion" (S_0) as a supernatant dispersion of supersaturated suspension of GNRs in THF. S_0 is obtained by deeply sonicating the supersaturated suspension and carefully taking the supernatant avoiding undispersed GNR particles at the bottom. S_0 is diluted with different amounts of THF to make an intermediate dispersion with varying concentrations. Since THF is slightly corrosive for the ESD components, the dispersion is further diluted 10 times with acetonitrile (CH_3CN) to obtain the dispersion that is actually used for ESD. We used two different concentrations composed by the following fractions, keeping the total volume constant:

S_1 = 1 (S_0) : 9 (THF) : 90 (CH_3CN)
S_2 = 1 (S_0) : 99 (THF) : 900 (CH_3CN)

After the dilution, dispersions was sonicated once more for at least 10 minutes at 40 °C in order to reduce the formation of GNR aggregates. In early tests we have also used methanol instead of acetonitrile, but in this case it was quite difficult to maintain

good dispersion and the deposition needed to be done immediately after sonication. The quantity of deposited material was controlled by the concentration of the dispersions and the time of deposition, since the rate of the syringe pump was kept constant. In the following, the quantity of deposited material is expressed in *ml* of sprayed dispersion. In our experiments the time of deposition ranged between 10 sec to 40 minutes, suggesting that this approach is a rather fast and efficient way to prepare films of GNRs on different types of substrates.

2.3 Surface techniques

The GNR film morphology has been firstly visualized by means of an optical microscope (Olympus-BX51M, see Supplementary Information).
SEM images were taken by using a Carl Zeiss Σigma microscope equipped with the GEMINI column (the typical acceleration voltage we used was 2kV).
We used a Veeco Multi Mode Nano Scope IIIa AFM tuned in tapping mode, while the STM images were taken by an Omicron UHV VT STM system.
Raman spectra have been collected by using a Jobin Yvom LabRAM with an integrated optical microscope, through which we could select the area to be illuminated. We used a laser's wavelength λ = 632.81 nm and the diameter of the spot was ≈ 1 μm in our typical configuration.

3. Results

3.1 Investigation by Raman Spectroscopy.

Raman spectroscopy is an efficient tool for studying carbon-based materials [26]. In particular the G peak at ~1600 cm^{-1} (related to the in-plane optical phonon branch and therefore is found in all carbon allotropes with sp^2 hybridization) and the D peak at ~1300 cm^{-1} (which is related to a second order process, in which out-of-plane optical phonons scatter with a defects) are the main fingerprints normally used to identify GNRs [27-30]. A careful analysis of their shape would allow to get further information about the GNR edges [28] and other features. We have simply performed a comparative study of these two peaks to get semi-quantitative information on the

quantity of deposited carbon material. A similar approach has been previously employed to study the deposition of carbon nanotubes and the growth of hydrogenated diamond-like carbon films prepared by plasma deposition [31, 32]. The background signal due to residual solvent or amorphous material was estimated and subtracted before the measurements of the GNR-deposited samples. In general, the intensity of a Raman peak depends on the laser power, spot size and the penetration depth of the beam. We therefore took care to perform all the measurements in the same conditions and in a short period of time in order to avoid the perturbation induced by laser heating. Statistics over the deposited surface was also necessary to account for thickness inhomogeneity (see Supplementary Information for more details).

Fig. 3b and 3c show the trend of the G and D peaks intensity for different deposition conditions on Au/mica. The intensity of both the Raman peaks clearly scales with the quantity of deposited GNR as estimated by the deposition parameters. Similar trends are also obtained considering the area of the respective peaks (see Fig. S3 in Supplementary Information). By decreasing the quantity of deposited GNRs, intensity and areas of both G and D peaks get very small and close to the limit of sensitivity of our measurements that we roughly estimate to be close to 1 monolayer by comparison with other type of samples.

Within the conical shape approximation for the injected beam, a simple model that relates different deposition parameters states that the quantity of deposited GNR should be proportional to:

$$Vs \cdot t \cdot C \cdot d^{-2}$$

where Vs = syringe-pump velocity (ml/min), t = time of deposition (min), C = concentration (a.u.), d = capillary – substrate distance (cm). We could verify that this simple relation holds as confirmed by the analysis of Raman peaks. In particular, we may notice that Raman peak scales by a factor 10 by increasing the concentration 10 times and that it approximately decreases a factor 4 by doubling the capillary – substrate distance (Fig. 3b and 3c).

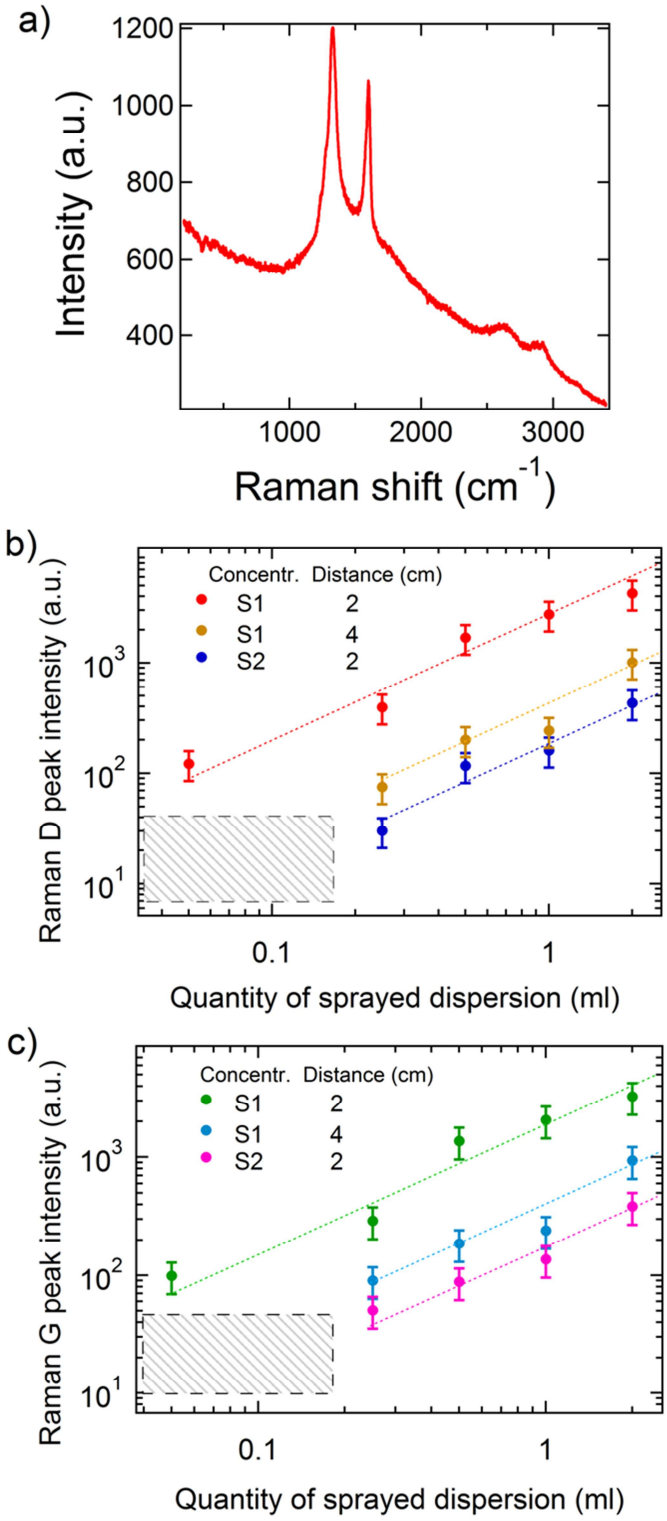

Figure 3: a) Typical Raman spectrum of a GNR film deposited by ESD on Au/mica. b) Intensity of the D peak as a function of the quantity of dispersion deposited for three different deposition conditions. c) Intensity of the G peak vs quantity of deposited dispersion.

3.2 Surface Investigation by Scanning Microscopies

Fig. 4 shows AFM images of a GNRs spot deposited on a Au/mica substrate. In this case, the deposition parameters were tuned to obtain one of the thinnest GNR films (see Fig. 3). A network of GNRs bundles is visible at the spot center (Fig. 4a) while we can recognize structures that can be associated to isolated GNRs with typical dimensions of ≈ 100 nm in length (Fig. 4b).

Similar results have been obtained by depositing GNRs also on the insulating SiO_2 substrate. Large substrate areas (200 μm wide) are homogenously covered by GNRs aggregates: an optical image of 0.25 ml of solution sprayed on a 300 nm thickness of SiO_2 surface over a Si bulk is shown in Fig. 5a. The formation of GNRs aggregates is confirmed by Raman spectra (Fig. 5b) whose intensity at the D and G peaks is very strong on purple spots. On the other hand, in the white shadows the Raman signal is much less intense (Fig. 5c) and it almost disappears (but still detectable) in the blue areas of the optical image. Both the SEM and AFM images better display the morphology of these aggregates, which is probably determined by the slow evaporation of residual solvent.

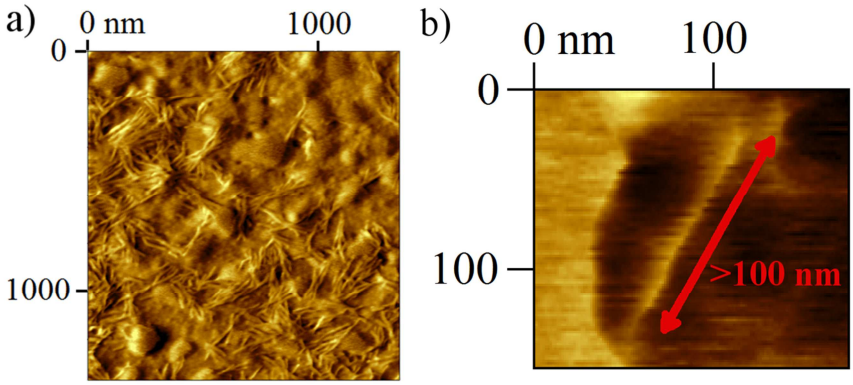

Figure 4: AFM images of GNRs deposited by ESD on Au/mica. a) Uniform distribution of aggregates and bundles of GNRs are visible for deposition with sufficiently high concentration (deposition conditions: 0.05 ml of S_1 on Au/mica, distance between capillary and substrate d = 2 cm). b) Isolated flat GNR with typical length of one hundred of nm are also visible in peripheral zones of the substrate and for lowest concentration density.

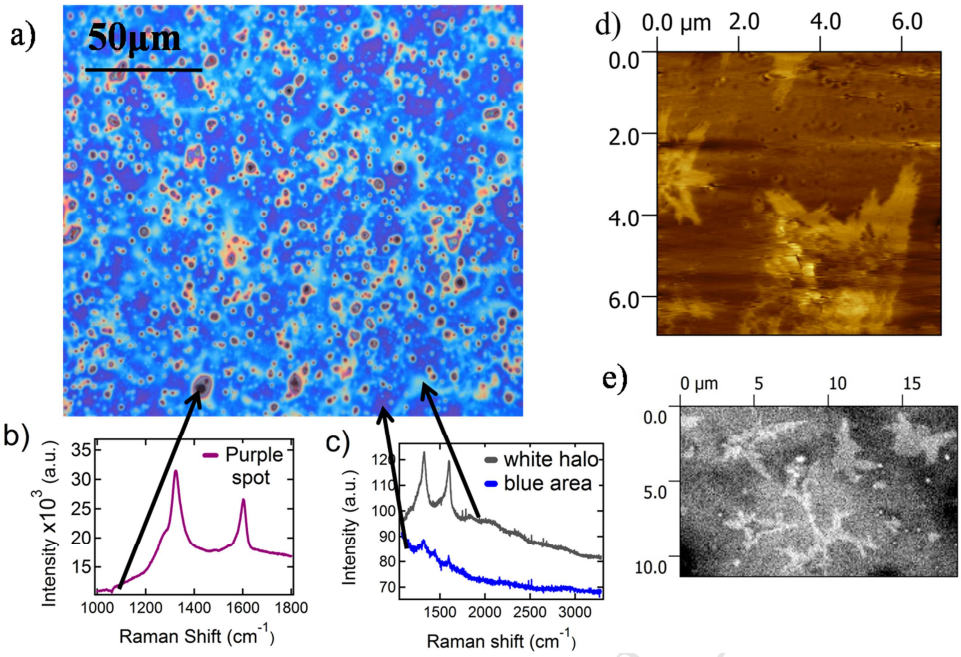

Figure 5: Images of GNRs deposited on SiO_2 . a) optical image (Magnification 100×) of GNRs deposited by ESD on SiO_2 (deposition parameters: 0.25 ml of S_1, d=4 cm) b) Typical Raman spectrum on the purple spots present on the substrate. c) Typical Raman spectrum on the white regions that surround the purple spots (grey spectrum) and on the blue areas (blue spectrum). d) AFM phase image of the aggregates of GNRs on SiO_2 . e) SEM image (Magnification =1200×) of GNRs aggregates on SiO_2 .

To further investigate the GNR film morphology we also took of STM images. In this case Au(111) surface, previously cleaned by sputtering/annealing procedure, was used in order to ensure good tunneling conditions. To find isolated GNR we inspected the external part of the Au(111) substrate, where the sprayed jet was less intense and the probability to form GNRs bundles is minor. STM images show that GNRs tend to accumulate at the edges of Au(111) terraces. Figure 6 shows a typical case: the height of white stripes is 0.4 nm above the gold steps while the lateral size of these 1D assembling ranges from 5 to 10 nm as estimated by STM, consistently with what expected by considering the lateral alkyl chains (4.15 nm) and by taking into account the image convolution with our tip.

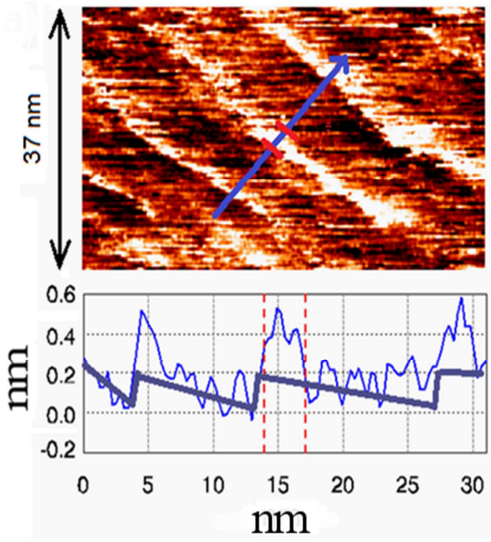

Figure 6: STM image of GNR deposited by ESD and situated in proximity of the Au(111) terraces (deposition conditions: 0.25 ml of S_1, d = 4 cm. STM setting: tunneling current = 0.1 nA, Tip voltage = -2 V). Notice the presence of extra peaks in the profile (0.4 nm above the height of the terrace) corresponding to the white stripes in the STM image.

3.3 Fabrication and characterization of three terminal device

To test the effectiveness of the ESD method for the realization of GNR-based electronic devices, we deposited the GNRs on graphitic electrodes on top of a 300-nm-thick SiO_2 substrate, using an underlying doped silicon to make a metallic back gate. The graphitic electrodes were prepared using the electro-burning process as described in details in Ref. [33]. Briefly, multilayer graphene flakes are mechanically exfoliated on the substrate and Cr/Au contacts (typically spaced 1 to 6 μm one to another, see Fig.7a) are then fabricated by electron beam lithography (EBL). A physical gap is then opened in the graphitic channel by the electro-burning process, setting the parameters to obtain an aperture of the order of ~10-50 nm. The effective opening of the gap was checked by the *I-V* characteristics taken after the electro-burning process, finding no measurable current in the range of –2V to +2V (Fig.7b). Then, we deposited GNRs by ESD on the whole substrate and measured again the conductance of the devices. The quantity of

sprayed solution (1 ml) makes reasonable the probability to get GNRs in the region of the gap (Fig. 7a). To have an idea of the production yield, on a chip with initially ~10 electro-burned devices, two of them show a significant increase of conductivity after the GNRs deposition (Fig. 7b).

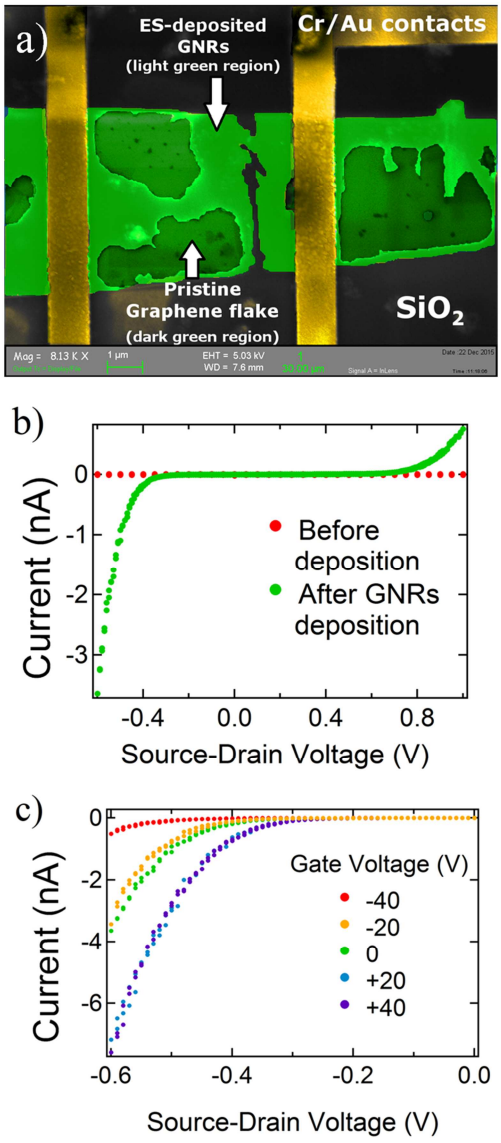

Figure 7: a) SEM image of graphitic contacts made by the electro-burning process [33] on which we deposited 1 ml of the dispersion S_1. The yellow stripes are Cr/Au contacts patterned by EBL. The graphene flake is colored in green: the dark green area is pristine graphene, while the light green is due to the ESD of GNRs. Part of the ES-deposited GNRs film bridging the gap between the two graphitic electrodes is clearly visible. b) I-V characteristics of an electro-burned device before and after the

deposition of GNRs through ESD. c) I-V characteristics for different values of the gate voltage.

To get reproducible *I-V* characteristics, an annealing (10 hours at 400 K) in vacuum (10^{-7} mbar) was necessary: it is likely that this makes the GNR film more stable on the surface, improving the electrical contact with the graphitic electrodes. After this annealing, the source-drain current I_{SD} is in the nA range for V_{SD} =0.5 V, significantly higher than what reported for drop casted GNR [8]. Non linear I-V curve suggests presence of an effective Schottky barrier. The conduction channel is composed by disordered aggregates of GNRs and the effective Schottky barrier here is due to both the ribbon-ribbon junctions and the contact resistance at the interface with the electrodes. Notice however that the resistance of the device ($10^8\ \Omega$) is one order of magnitude lower than what reported in literature [8] for similar devices with GNRs deposited by drop-casting but using Ti/Au contacts.

Interestingly, such *I-V* characteristics show a pronounced gate dependence (Fig. 7c), with a current on/off ratio as high as 5, higher than what reported for this type of solution-synthesized GNRs [8,9], proving the effectiveness of the ESD as fabrication method.

We found that our devices have an n-type behavior in the gate range experimentally accessible (Fig. S5 in Supplementary Information). The n-type behavior was also reported for GNRs grown under ultra-high vacuum and contacted by Pd electrodes [34] so the characteristic of our devices is not surprising although in different conditions one may also have p-doped devices [8,9]. Bipolar behavior is expected but in our case we would need values of the gate voltage beyond safe experimental conditions.

We can estimate the electron mobility μ following the procedure for FET in the linear region [35] and we found values ranging from $1{\cdot}10^{-3}$ to $1{\cdot}10^{-2}$ $cm^2\ V^{-1}\ s^{-1}$ (See Supplementary Information for more details). As expected, these values are small for homogeneus semiconductors and more similar to what found in organic electronics. They suggest that the conducting channel of our device is made of GNR aggregates - consistently with AFM and SEM images - whose conductivity is dominated by junction between GNRs.

4. Discussion and Conclusions

In this work we have used a simple setup to spray ultra-long solution-synthesized GNRs dispersed in organic solvents. This approach allowed us to circumvent intrinsic and technical difficulties (*e.g.* transfer of GNR on non conducting substrate, evaporation of large mass molecules etc.) that are limiting the use of GNR in electronics. The use of combined analysis allowed us to show that ESD is an efficient way to deposit GNRs on any type of substrates (we tested both metallic Au/mica and non conducting SiO_2), and to cover large area, as shown by optical microscopy, SEM and AFM on different scales (μm^2 to cm^2). We used semi-quantitative analysis of the G and D Raman peaks to quantify the amount of deposited material and show that it is possible to control the quantity of material deposited through the feeding electrospray source. Three terminal electronic devices have been successfully fabricated by electrospray GNRs onto a SiO_2 substrate with graphitic electrodes. *I-V* characteristics show finite current (nA at V_{SD}=0.5V) through the GNR channel and dependence to the gate voltage. Overall, these results show that ESD is a fast deposition technique that represents a valid alternative to drop casting for deposition in ambient conditions.

Further improvements are readily visible adopting suitable technical solutions. For instance, GNRs film homogeneity can be further improved by placing the substrate more distant from the spraying capillary. Additional improvement can potentially be obtained by depositing in a chamber with differential pressure: this may facilitate formation of smaller droplets and improve homogeneity over large surfaces. In commercial mass spectrometers, such chamber is placed off axis and after selection of charged molecules and, in the case of GNR, its use results in a drastic reduction of deposition rates. This can be suitable for fabrication of devices comprising single GNR. Alternatively different designs with substrate facing the capillary after chambers with differential pressure may allow efficient deposition also in UHV conditions.

Another interesting parameter of ESD is the application of high potential $\Delta V=V_c-V_s$ between the capillary and the substrates. This has essentially two roles: firstly

it ionizes the droplets thus facilitating their dispersion; secondly it charges GNRs. The latter process is necessary to accelerate the GNRs and to select their masses if spectrometer is used. Yet, because of the large mass of GNRs, this process is scarcely effective and it can be exploited only with a dedicated apparatus. Nevertheless, charged GNRs tend to repulse each other and to better stick on surface. Thus, even if electromagnetic lenses are not used for mass selection, the use of charging potential can help in depositing isolated GNRs on substrate and this can be a further parameter to be controlled.

Acknowledgements.

This work has been partially supported by European Community through the FET-Proactive Project *"MoQuaS"*, contract N.610449, and Graphene Flagship (No. CNECT-ICT-604391), by the Italian Ministry for Research (MIUR) through the FIR grant RBFR13YKWX, by the European Research Council grant on NANOGRAPH, and by DFG Priority Program SPP 1459.

References.

[1] http://www.futuremarketsinc.com/graphene-market/

[2] Han MY, Özyilmaz B, Zhang Y, Kim P. Energy Band-Gap Engineering of Graphene Nanoribbons. Phys Rev Lett 2007;98(20):206805. http://dx.doi.org/10.1103/PhysRevLett.98.206805

[3] Kosynkin DV, Higginbotham AL, Sinitskii A, Lomeda JR, Dimiev A, Price BK. Longitudinal unzipping of carbon nanotubes to form graphene nanoribbons. Nature 2009;458(7240):872-6. doi: 10.1038/nature07872

[4] Cai J, Ruffieux P, Jaafar R, Bieri M, Braun T, Blankenburg S, et al. Atomically precise bottom-up fabrication of graphene nanoribbons. Nature 2010;466:470-6. doi:10.1038/nature09211

[5] Baringhaus J, Ruan M, Edler F, Tajeda A, Sicot M, Taleb-Ibrahimi A, et al. Exceptional ballistic transport in epitaxial graphene nanoribbons. Nature 2014;506:349-54. doi:10.1038/nature12952

[6] Narita A, Feng X, Hernandez Y, Jensen SA, Bonn M, Yang H, et al. Synthesis of structurally well-defined and liquid phase-processable graphene nanoribbons. Nat Chem 2014;6:126-32. doi:10.1038/nchem.1819

[7] Narita A, Wang X-Y, Feng X, Müllen K. New advances in nanographene chemistry. Chem Soc Rev 2015;44:6616-43. DOI: 10.1039/C5CS00183H

[8] Abbas AN, Liu G, Narita A, Orosco M, Feng X, Müllen K, et al. Deposition, Characterization, and Thin-Film-Based Chemical Sensing of Ultra-long Chemically Synthesized Graphene Nanoribbons. J Am Chem Soc 2014;136(21):7555–8. DOI: 10.1021/ja502764d

[9] Zschieschang U, Klauk H, Müeller IB, Strudwick AJ, Hintermann T, Schwab MG, et al. Electrical Characteristics of Field-Effect Transistors based on Chemically Synthesized Graphene Nanoribbons. Adv Electron Mater 2015;1(3):1400010. doi: 10.1002/aelm.201400010 (2015)

[10] Konnerth R, Cervetti C, Narita A, Feng X, Müllen K, Hoyer A, et al. Tuning the deposition of molecular graphene nanoribbons by surface functionalization. Nanoscale 2015;7:12807-11. DOI: 10.1039/C4NR07378A

[11] Kitching KJ, Lee H-N, Elam WT, Johnston E, MacGregor H, Miller RJ, et al. Development of an electrospray approach to deposit complex molecules on plasma modified surfaces. Rev Sci Instrum 2003;74(11):4832-9. DOI: 10.1063/1.1618013

[12] Rietveld IB, Kobayashi K, Yamada H, Matsushige K. Electrospray Deposition, Model, and Experiment: Toward General Control of Film Morphology. J Phys Chem B 2006;110(46):23351-64. DOI: 10.1021/jp064147+

[13] Rauschenbach S, Stadler FL, Lunedei E, Malinowski N, Koltsov S, Costantini G, et al. Electrospray ion beam deposition of clusters and biomolecules. Small 2006;2(4):540–7. DOI: 10.1002/smll.200500479

[14] Rauschenbach S, Vogelgesang R, Malinowski N, Gerlach JW, Benyoucef M, Costantini G, et al. Electrospray Ion Beam Deposition: Soft-Landing and Fragmentation of Functional Molecules at Solid Surfaces. ACS Nano 2009;3(10):2901–10. DOI: 10.1021/nn900022p

[15] Hinaut A, Pawlak R, Meyer E, Glatzel T. Electrospray deposition of organic molecules on bulk insulator surfaces. Beilstein J Nanotechnol 2015;6:1927–34. doi:10.3762/bjnano.6.195

[16] Ouyang Z, Takáts Z, Blake TA, Gologan B, Guymon AJ, Wiseman JM, et al. Preparing Protein Microarrays by Soft-Landing of Mass-Selected Ion. Science 2003;301:1351. DOI: 10.1126/science.1088776

[17] Satterley CJ, Perdigão LMA, Saywell A, Magnano G, Rienzo A, Mayor LC, et al. Electrospray deposition of fullerenes in ultra-high vacuum: in situ scanning tunneling microscopy and photoemission spectroscopy. Nanotechnology 2007;18:455304 doi:10.1088/0957-4484/18/45/455304

[18] Saywell A, Magnano G, Satterley CJ, Perdigão LMA, Champness NR, Beton PH et al. Electrospray Deposition of C_{60} on a Hydrogen-Bonded Supramolecular Network. J Phys Chem C2008;112(20):7706–9. DOI: 10.1021/jp7119944

[19] O'Shea JN, Taylor JB, Swarbrick JC, Magnano G, Mayor LC, Schulte K. Electrospray deposition of carbon nanotubes in vacuum. Nanotechnology 2007;18:035707. doi:10.1088/0957-4484/18/3/035707

[20] Saywell A, Britton AJ, Taleb N, Giménez-López MC, Champness NR, Beton PH, et al. Single molecule magnets on a gold surface: in situ electrospray deposition, x-ray absorption and photoemission. Nanotechnology 2011; 22: 075704. http://dx.doi.org/10.1088/0957-4484/22/7/075704

[21] Corradini V, Cervetti C, Ghirri A, Biagi R, del Pennino U, Timco GA, et al. Oxo-centered carboxylate-bridged trinuclear complexes deposited on Au(111) by a mass-selective electrospray. New J Chem 2011; 35:1683–1689. DOI: 10.1039/c1nj20080a

[22] Saywell A, Magnano G, Satterley CJ, Perdigão LMA, Britton AJ, Taleb N, et al. Self-assembled aggregates formed by single-molecule magnets on a gold surface. Nat Commun 2010;1:75. doi:10.1038/ncomms1075

[23] Erler P, Schmitt P, Barth N, Irmler A, Bouvron S, Huhn T, et al. Highly Ordered Surface Self-Assembly of Fe_4 Single Molecule Magnets. Nano Lett 2015;15(7):4546−52. DOI: 10.1021/acs.nanolett.5b01120

[24] Bromann K, Félix C, Brune H, Harbich W, Monot R, Buttet J, et al. Controlled Deposition of Size-Selected Silver Nanoclusters. Science 1996;274(5289):956-8. DOI: 10.1126/science.274.5289.956

[25] Jaworek A. Electrospray droplet sources for thin film deposition. J Mater Sci 2007;42:266–97. DOI 10.1007/s10853-006-0842-9

[26] Tuinstra F, Koenig JL, Raman Spectrum of Graphite. J Chem Phys 1970;53:1126. doi: 10.1063/1.1674108

[27] Ferrari AC, Basko DM. Raman spectroscopy as a versatile tool for studying the properties of graphene. Nat Nanotechnol 2013;8:235-46. doi:10.1038/nnano.2013.46

[28] Casiraghi C, Hartschuh A, Qian H, Piscanec S, Georgi C, Fasoli A, et al. Raman Spectroscopy of Graphene Edges. Nano Lett 2009;9(4):1433-41. DOI: 10.1021/nl8032697

[29] Zhou J, Dong J. Vibrational property and Raman spectrum of carbon nanoribbon. Appl Phys Lett 2007;91:173108. doi: 10.1063/1.2800796

[30] Gillen R, Mohr M, Maultzsch J. Raman-active modes in graphene nanoribbons. Physica Status Solidi B 2010;247(11-12):2941-4. DOI10.1002/pssb.201000354

[31] Salzmann CG, Chu BTT, Tobias G, Llewellyn SA, Green MLH. Quantitative assessment of carbon nanotube dispersions by Raman spectroscopy. Carbon 2007;45(5):907-12. doi:10.1016/j.carbon.2007.01.009

[32] Singha A, Ghosh A, Roy A, Ray NR. Quantitative analysis of hydrogenated diamondlike carbon films by visible Raman spectroscopy. J Appl Phys 2006;100:044910. doi: 10.1063/1.2219983

[33] Candini A, Richter N, Convertino D, Coletti C, Balestro F, Wernsdorfer W, et al. Electroburning of few-layer graphene flakes, epitaxial graphene, and turbostraticgraphene discs in air and under vacuum. Beilstein J Nanotechnol 2015;6:711–9. doi: 10.3762/bjnano.6.72

[34] Bennett PB, Pedramrazi Z, Madani A, Chen Y-C, de Oteyza DG, Chen C, et al. Bottom-up graphene nanoribbon field-effect transistors. Appl Phys Lett 2013;103:253114. doi: 10.1063/1.4855116

[35] Radisavljevic R, Radenovic A, Brivio J, Giacometti V, Kis A. Single-layer MoS_2 transistors. Nat Nanotechnol 2011;6:147–50. doi:10.1038/nnano.2010.279